
This is an electronic reprint of the original article.
This reprint may differ from the original in pagination and typographic detail.

Author(s): Hakonen, Pertti J. & Nummila, K. K. & Vuorinen, R. T.
Title: Spin dynamics in highly polarized silver at negative absolute temperatures
Year: 1992
Version: Final published version

Please cite the original version:

Hakonen, Pertti J. & Nummila, K. K. & Vuorinen, R. T. 1992. Spin dynamics in highly polarized silver at negative absolute temperatures. *Physical Review B*. Volume 45, Issue 5. 2196-2200. ISSN 0163-1829 (printed). DOI: 10.1103/physrevb.45.2196

Rights: © 1992 American Physical Society (APS). This is the accepted version of the following article: Hakonen, Pertti J. & Nummila, K. K. & Vuorinen, R. T. 1992. Spin dynamics in highly polarized silver at negative absolute temperatures. *Physical Review B*. Volume 45, Issue 5. 2196-2200. ISSN 0163-1829 (printed). DOI: 10.1103/physrevb.45.2196, which has been published in final form at <http://journals.aps.org/prb/abstract/10.1103/PhysRevB.45.2196>.

Spin dynamics in highly polarized silver at negative absolute temperatures

P. J. Hakonen, K. K. Nummala, and R. T. Vuorinen

Low Temperature Laboratory, Helsinki University of Technology, 02150 Espoo, Finland

(Received 6 August 1991)

We have studied the spin dynamics of highly polarized silver nuclei at negative absolute temperatures up to inverted polarizations $p \approx -70\%$. The measured NMR spectra at $B=0.4$ and 0.8 mT display a clear inverted suppression-enhancement effect, arising from an interaction between the two spin species, ^{107}Ag and ^{109}Ag . The averaged interaction-field description accounts well for the intensity ratio of the isotopic NMR lines. The frequency difference of the absorption maxima has been used to study the merging and repulsion of the NMR modes at large negative polarizations. At $B=0.2$ mT, our spectra display only a single exchange-merged line, indicating that the two isotopes act as like spins. The transition from a single NMR line to two separate lines proceeds in a similar fashion as at positive temperatures. No effects attributable to the tendency of ferromagnetic alignment of spins at $T < 0$ were observed.

I. INTRODUCTION

Spin dynamics in highly polarized metals has been studied previously in copper by Ekström *et al.*,¹ in thallium by Eska and Schuberth,^{2,3} and in silver by Oja, Annila, and Takano.^{4,5} Characteristic to these metals is that they contain two stable isotopes with slightly different gyromagnetic ratios γ , which leads to interesting phenomena owing to coupling between the two isotopic NMR lines in small magnetic fields. Ekström *et al.*¹ observed the so-called suppression-enhancement effect of the NMR lines where the peak at higher-resonance frequency is enhanced at the expense of the line at the smaller frequency. They used the equations of motion for the two magnetizations, including the molecular interaction fields, to relate the measured intensity ratio of the isotopic lines to the interaction parameter R [see Eq. (3) below]; this scheme was also applied by Oja, Annila, and Takano⁵ who obtained $R = -2.5 \pm 0.5$ for silver.

The studies on thallium^{2,3} have displayed more puzzling behavior than silver or copper. Thallium has a large ferromagnetic exchange interaction, on the basis of which ferromagnetic ordering has been expected.² The measurements have revealed a splitting, even to multiple peaks, of the NMR line at high polarizations. This has been interpreted as trapping of spin-wave modes on impurities formed by the less abundant isotope (30 at. % of ^{203}Tl) in the matrix of ^{205}Tl .⁶ Another explanation was proposed by Oja, Annila, and Takano⁷ who showed, using second-order perturbation theory, that a resplitting of a merged NMR line is possible at large polarizations owing to competition between the merging of NMR lines by thermal fluctuations and the ordinary repulsion of energy levels, since these two opposing tendencies have different polarization dependencies. Oja, Annila, and Takano⁵ have also made experiments to study these phenomena in silver up to polarizations of 70%.

We have extended these studies into the range of negative absolute temperatures where inverted polarizations

up to $p \approx -70\%$ have been reached. Nuclear magnetism and magnetic ordering at negative absolute temperatures have been studied in insulators.⁸ Similar investigations are much more involved in metals, first because it takes more effort to achieve high polarizations and, second, because eddy currents make the production of a large inverted population difficult.

At negative temperatures an isolated spin system tries to maximize its energy instead of minimizing it. This means that the antiferromagnetic exchange interaction in silver prefers ferromagnetic alignment of spins at negative temperatures. This tendency might influence the merging of the NMR lines and make the behavior of silver at $T < 0$ resemble more the behavior in thallium.

Our results indicate, however, no drastic difference in the merging behavior of silver at positive and negative absolute temperatures. We find a clear inverted suppression enhancement at $T < 0$: The peak at the lower frequency is enhanced, while the peak at higher frequency is suppressed. This observation is in accordance with the averaged interaction field model of Ref. 1 when the magnetizations are inverted. By comparing the measured NMR frequencies with the calculated modes, we deduce the magnitude of the merging term, which is in accordance with the calculations by Karimov and Shchegolev⁹ and by Oja, Annila, and Takano.⁷

Natural silver has two species with spin $S = \frac{1}{2}$: 51.8 at. % of ^{107}Ag and 48.2 at. % of ^{109}Ag . These isotopes also have slightly different gyromagnetic ratios, $\gamma_{107}/2\pi = 1.723$ MHz/T and $\gamma_{109}/2\pi = 1.9807$ MHz/T. The Hamiltonian in silver is a sum of the dipolar and indirect Ruderman-Kittel exchange interactions, in addition to the Zeeman energy, viz.,

$$H = H_{\text{dip}} + H_{\text{ex}} + H_Z \\ = (\mu_0/8\pi)\hbar^2 \sum_{i,j} \gamma_i \gamma_j \mathbf{I}_i \cdot \vec{\mathbf{A}}_{ij} \cdot \mathbf{I}_j - \hbar \mathbf{B} \cdot \sum_i \gamma_i \mathbf{I}_i, \quad (1)$$

where B is the external magnetic field, μ_0 is the vacuum

permeability, and the spin-spin interaction matrix, contributing to H_{dip} and H_{ex} is

$$A_{ij}^{\mu\nu} = r_{ij}^{-3} [\delta_{\mu\nu} - 3(\hat{r}_{ij})_{\mu}(\hat{r}_{ij})_{\nu}] - \frac{1}{2} J_{ij} \delta_{\mu\nu} / [(\mu_0/8\pi)\hbar^2 \gamma_i \gamma_j] . \quad (2)$$

The dominating spin-spin energy is the nearest-neighbor exchange interaction whose magnitude may be estimated from the NMR experiment by Poitrenaud and Winter,¹⁰ using a linewidth analysis which yields $|J|/\hbar = 26.5$ Hz. The sign of J is negative, as determined by Oja, Annala, and Takano⁴ in cross-relaxation experiments; i.e., the interaction is antiferromagnetic. Recently, similar values have also been obtained from first-principles band-structure calculations.^{11,12}

According to mean-field theory, the effective field B_{eff} , seen by individual spins when $B \gg B_{\text{loc}} = 35$ μT , can be written as

$$B_{\text{eff}} = B + \mu_0(R + L - D)\rho M_{\text{sat}} , \quad (3)$$

where $R = \sum_i J_{ij} / (\mu_0 \rho \gamma^2 \hbar^2)$ and $M_{\text{sat}} = \rho \gamma \hbar / 2$; ρ is the number density of atoms and γ is the weighted average of the two isotopic γ_i 's. The dipolar interaction contributes to the Lorentz and shape-dependent demagnetization fields, which give rise to the factors $L = \frac{1}{3}$ and D , respectively. B_{eff} determines the NMR frequencies of the noninteracting isotopic NMR lines in Eq. (6) below.

II. EXPERIMENTAL TECHNIQUES

Our silver sample consists of 48 polycrystalline foils with dimensions $8 \times 0.025 \times 65$ mm³, oriented along the x , y , and z directions, respectively. The nominal purity is 99.99+%. Every foil was folded once (to 4 mm width) and grouped with six others into a structure where each U -shaped foil ties two adjacent foils together to form a rigid structure. A 7- μm layer of SiO_2 powder was used to keep the foils electrically isolated from each other. This construction resulted in a vibration-free, rigid structure whose demagnetization factors, however, were not very well defined and had to be found experimentally.

The static field along the x or y axis is produced by two superconducting saddle-shaped coils (lengths 60 and 65 mm); B_z is generated with a solenoid 70 mm long. All coils, wound of 50- μm multifilamentary NbTi superconducting wire, are located on a coil former ($\phi = 14$ mm) inside a brass radiation shield ($\phi = 16.5$ mm). The latter has four cuts symmetrically along its length to reduce eddy currents which could prevent rapid changes in the experimental magnetic field. The astatically wound pickup coil is oriented along the z axis. The NMR spectra were measured by sweeping the frequency in a manner originally described by Ehnholm *et al.*¹³ The data reported by us were taken with the static field along the y axis, perpendicular to the foils, aiming at the symmetric situation $D_y = 1$ and $D_x = D_z = 0$, which would be advantageous for the data analysis. However, this was not quite true for our sample: By measuring NMR shifts due to small polarization at 0.1–0.2-mT fields in the x and y directions, we obtained $D_x:D_y \approx 1:3$, and therefore we estimate $D_x = 0.25$, $D_y = 0.75$, and $D_z = 0$.

The experiments were performed in the double-stage nuclear demagnetization apparatus in Helsinki.¹⁴ Thermometry was based on the susceptibility of ¹⁹⁵Pt in platinum wires, calibrated against Be and W superconducting fixed points. For details of the cooling process and experimental techniques, we refer to Ref. 15. The demagnetization procedure in these experiments was slightly modified: We employed degaussing of the second magnet ($+7.4$ T \rightarrow -0.1 T \rightarrow $+0.02$ T \rightarrow 0) to guarantee proper operation of the superconducting quantum interference device (SQUID) measurement system, susceptible to flux creep and vibrational noise in the presence of a remnant field. Fortunately, this degaussing scheme did not substantially decrease the maximum initial polarization of $p = 85\%$ achieved in the experiments.

Since all averaged interaction fields are proportional to the polarization of the nuclear spins, the determination of this quantity is important for our studies. The polarization of the silver spin system was found from the measured area of the NMR absorption signal, at fields $B \gg B_{\text{loc}}$, according to

$$p = A \int_0^\infty \chi''(f) df , \quad (4)$$

where A is a calibration constant. We used a static measuring field of 0.20 mT because then the separate identity of the ¹⁰⁷Ag and ¹⁰⁹Ag spins is largely lost and there is only one sharp line, which is easy to integrate [see Fig. 1(a)]. The calibration, described fully in Ref. 15, was made around 1 mK, where the initial polarization of silver nuclei could be calculated reliably from the measured temperature.

The production of negative absolute temperatures, which requires a population inversion of energy levels, was performed by a rapid reversal of the solenoidal magnetic field B_z in a time shorter than the spin-spin relaxation time $\tau_2 \approx 10$ ms. The experimental coil system and radiation shield were especially designed to reduce eddy currents, which were supposed to have been the main obstacle in previous attempts of polarization inversion.^{16,17} The field used in the rapid reversal was about 400 μT . Our best inversion efficiency was 90%, which was obtained at small initial polarizations of the order of $p = 30\%$. At the initial polarization of $p \approx 85\%$, the efficiency was typically 60–75%. Therefore, polarizations at $T < 0$ were limited to $p \approx -65\%$.

During an experiment, the spin system continuously “cooled down” owing to the spin-lattice relaxation; the electronic temperature of 0.2 mK yields $\tau_1 \approx 10$ h. This relaxation rate is small enough so that a few NMR spectra at 0.2 and 0.4 (0.8) mT could be measured without any noticeable change in polarization. After each set of spectra, the system was heated up by a 5–20-sec rf pulse, applied at $B = 0$, which changed the polarization of the spins by about 10–20%.

III. RESULTS AND DISCUSSION

Figure 1 displays examples of NMR line shapes measured at 0.2, 0.4, and 0.8 mT. The curves at 0.2 mT show only a single line, which indicates that the two isotopes act like equals and produce a narrow, exchange-merged

NMR line, as at positive temperatures. The line shapes at 0.4 and 0.8 mT display a clear inverted suppression-enhancement effect: The NMR peak of ^{107}Ag at low frequencies is enhanced at the expense of the high-frequency ^{109}Ag line. This behavior is more pronounced at the 0.4-mT field where the NMR peaks start to overlap, which increases the interaction of the two modes. Line shapes

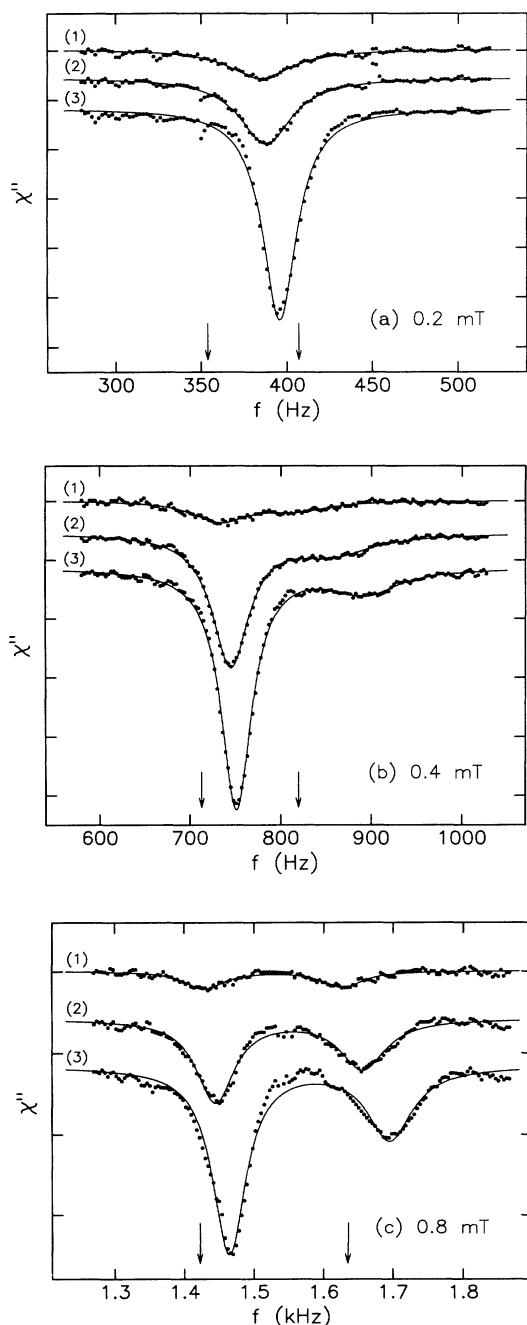


FIG. 1. NMR absorption χ'' (arbitrary units) as a function of frequency measured at different values of the external magnetic field. (a) $B = 0.205$ mT; (1) $p = -0.173$, (2) $p = -0.286$, and (3) $p = -0.683$. (b) $B = 0.411$ mT; (1) $p = -0.056$, (2) $p = -0.343$, and (3) $p = -0.485$. (c) $B = 0.822$ mT; (1) $p = -0.120$, (2) $p = -0.374$, and (3) $p = -0.683$. Solid curves are fits of Lorentzian lines.

were also measured at 0.3 mT up to $p = -50\%$. However, no abrupt changes were observed in our measurements which would correspond to splitting of the NMR line at $p > 40\%$ as observed by Eska and Schubert² in thallium with ferromagnetic exchange interaction.

The measured line shapes at 0.4 and 0.8 mT can be accounted for by the model developed by Ekström *et al.*¹ They treated all the spin-spin interactions by averaged fields and derived an equation, for the dynamic susceptibility,

$$\chi(\omega)^{-1} = \chi_0(\omega)^{-1} - (R + L - D_{\text{rf}}), \quad (5)$$

where $\chi_0(\omega)$ is the susceptibility of the noninteracting spin system in the field B_{eff} and D_{rf} represents the two equal demagnetization factors perpendicular to the external field. In our sample, with the static field along the y axis, perpendicular to the foils, this requirement is not fulfilled since $D_x \approx 0.25$ and $D_z \approx 0$, but the difference is so small compared with the magnitude of R that it may be neglected. We approximate $\chi_0(\omega)$ by the Lorentzian line shapes

$$\chi_0(\omega)^{-1} = \sum_k [(\omega_k - \omega) - i/\tau_2] / \chi_k \omega_k, \quad (6)$$

where the index k refers to the two isotopes, $\omega_k = \gamma_k B_{\text{eff}}$, and $\chi_k = \mu_0 p M_{k,\text{sat}} / B$. The solid lines in Fig. 1 exemplify the fits. The agreement is very good at 0.4 mT, whereas at 0.8 mT the measured line shapes fall off faster than the fits, indicating that the shapes are closer to Gaussian forms. The fits at small polarizations yield $\tau_2 = 6$ and 8 ms for ^{107}Ag and ^{109}Ag , respectively. The deviations from the reported values,¹⁸ 9.1 and 10.4 ms, are due to about 1% inhomogeneity of the static field.

The intensity ratio of the NMR absorption lines, I_{107}/I_{109} , was obtained by integrating the measured peaks separately. At 0.8 mT the integration was performed directly from the data, but at 0.4 mT Lorentzian lines were first fitted to the points and the curves then integrated. The result is displayed in Fig. 2 as a function of polarization. The solid curves have been calculated using Eqs. (5) and (6) with $R + L = -2$, $D_{\text{rf}} = 0$, and the demagnetization factor along the static field $D_y = 0.75$. The value for R was obtained from the frequency shifts to be discussed below; it is close to the value $R = -2.5 \pm 0.5$ obtained from NMR measurements at positive temperatures⁵ and from the susceptibility experiments.¹⁷ The agreement between the calculated curve and experimental points is very good at 0.8 mT. At 0.4 mT the theoretical curve falls below the data, which may be due to problems in separating the two isotopic peaks. On the whole the model by Ekström *et al.*¹ accounts well for the intensity ratio of the inverted suppression-enhancement effect at negative temperatures.

In order to study the merging and repulsion of the NMR modes at large negative polarizations, we have measured the frequency difference of the absorption maxima, $\Delta f = f_{109} - f_{107}$, which is displayed in Fig. 3 as a function of polarization. At 0.8 mT the maxima have been read directly from the data, whereas Lorentzian fits were again used at 0.4 mT to determine f_{109} more reli-

ably [see Fig. 1(b)]. The dashed lines in Fig. 3 show the frequency difference of the absorption maxima calculated from Eqs. (5) and (6) with the same parameters as in the case of the intensity ratio.

There is a clear difference between the dashed curves based on the model of Ekström *et al.*¹ and the measured frequency shift in Fig. 3. The fact that we are studying the frequency differences of the modes eliminates the possibility that shape-dependent interaction fields or remnant fields could be the origin. Therefore, the difference can be attributed to the merging term, caused by thermal fluctuations, which is not included in molecular-field theory. According to the second-order perturbation expansion by Oja, Annala, and Takano⁷ without the pseudo-dipolar interactions, the change in the angular frequency difference $2\pi(f_{109} - f_{107})$ owing to this term is of the form

$$\Delta\omega_m = -\frac{1}{4\hbar^2\Delta\gamma B}(1-p^2)\sum_j J_{ij}^2, \quad (7)$$

where $\Delta\gamma = \gamma_{109} - \gamma_{107}$ and where we have approximated the abundances of the two isotopes with 0.5; in the limit

$p \rightarrow 0$ this formula coincides with the result of Karimov and Shchegolev.⁹ The second-order p^2 expansion has also a repulsion term

$$\Delta\omega_r = +\frac{1}{8\hbar^2\Delta\gamma B}p^2\left[\sum_j J_{ij}\right]^2, \quad (8)$$

which, however, is already included in the internal field equations.

When the merging term of Eq. (7), with $\sum_i J_{ij}^2/\hbar^2 = 8430 \text{ Hz}^2$, is included,¹⁰ we obtain a fairly good agreement between theory and the measured Δf as displayed by the solid lines in Fig. 3. Unfortunately, since the value of R is not well known independently, we cannot conclude much from the experimental polarization dependence of the merging term: A constant value would fit our data almost equally well if the employed $R = -2.33$ were changed to be a little more negative. The present value has been selected as a compromise between the fits at 0.4 and 0.8 mT; slightly more weight was given to the latter set of data since the peaks are more clearly separated at 0.8 than at 0.4 mT.

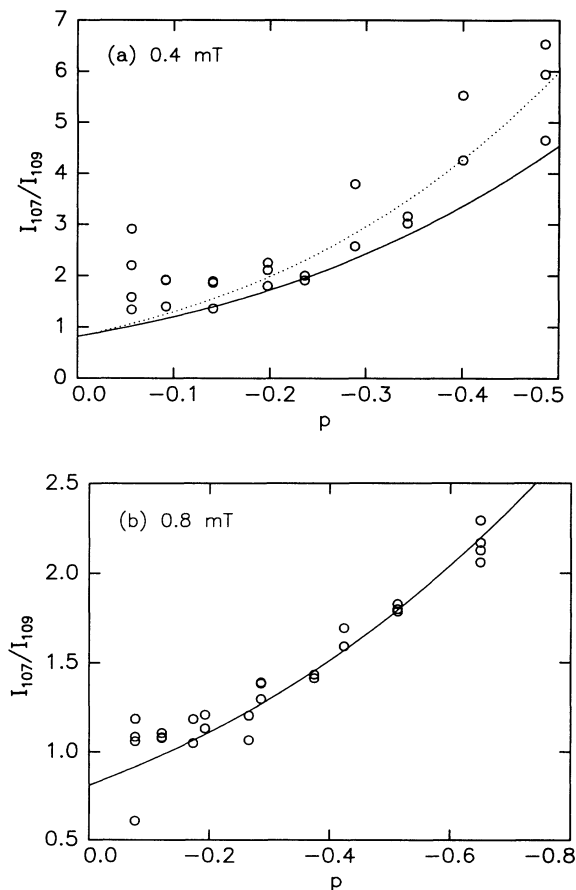


FIG. 2. Intensity ratio of the NMR absorption lines, I_{107}/I_{109} , as a function of polarization at (a) $B = 0.411 \text{ mT}$ and (b) $B = 0.822 \text{ mT}$. Solid curves are fits to Eqs. (5) and (6) with $R + L = -2.0$, dotted curve in (a) with $R + L = -2.5$; see text.

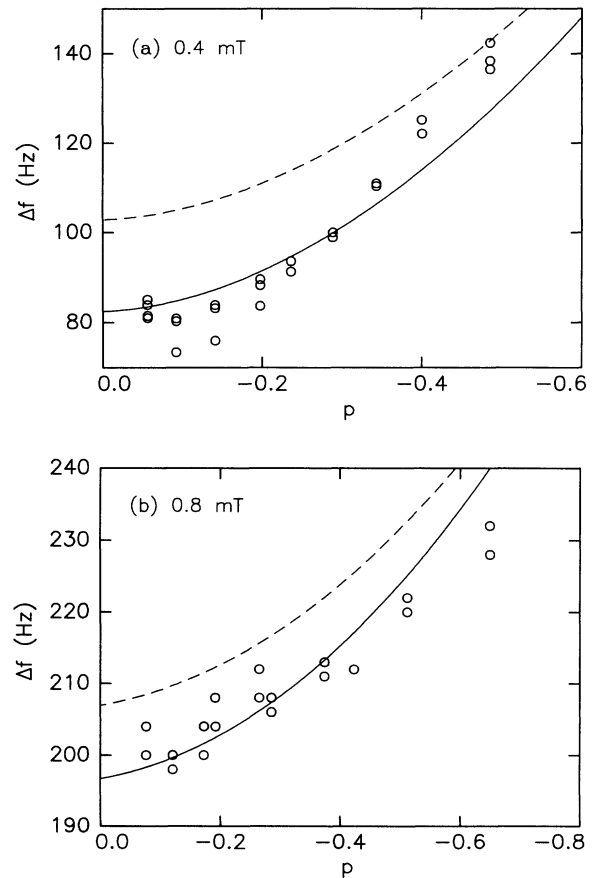


FIG. 3. Frequency difference of the absorption maxima, $\Delta f = f_{109} - f_{107}$, as a function of polarization at (a) $B = 0.411 \text{ mT}$ and (b) $B = 0.822 \text{ mT}$. Dashed curves are fits to Eqs. (5) and (6) with $R + L = -2.0$, and solid curves include the effect of the merging term in Eq. (7); see text.

IV. CONCLUSION

In summary, we have made detailed investigations of nuclear spin dynamics in a metal at $T < 0$. We have studied the transition from a single NMR line to two separate lines in silver at strong negative polarizations. The observed gradual transformation proceeds in a similar fashion as at positive temperatures,⁵ except that the role of the ^{107}Ag and ^{109}Ag nuclei are interchanged; the transformation can be accounted for by spin dynamics employing averaged interaction fields. Despite the fact that

the antiferromagnetic interaction results in a ferromagnetic tendency at $T < 0$, no effects were observed which would equal those observed in thallium with ferromagnetic exchange.^{2,3}

ACKNOWLEDGMENTS

We are grateful to I. Fomin, J. Kurkijärvi, O. V. Lounasmaa, and A. S. Oja for useful comments and discussions.

¹J. P. Ekström, J. F. Jacquinot, M. T. Loonen, J. K. Soini, and P. Kumar, *Physica B* **98**, 45 (1979).

²G. Eska and E. Schuberth, *Jpn. J. Appl. Phys.* **26**, Suppl. 3, 435 (1987).

³G. Eska, in *Symposium on Quantum Fluids and Solids—1989*, Proceedings of a conference on Quantum Fluids and Solids—1989, at the University of Florida, Gainesville, Florida, April 24–28, 1989, edited by G. G. Ihas and Y. Takano, AIP Conf. Proc. No. 194 (AIP, New York, 1989), p. 316.

⁴A. S. Oja, A. J. Annala, and Y. Takano, *Phys. Rev. Lett.* **65**, 1921 (1990).

⁵A. S. Oja, A. J. Annala, and Y. Takano (unpublished).

⁶D. Rainer, I. Fomin, and G. Eska (unpublished).

⁷A. S. Oja, A. J. Annala, and Y. Takano, *Phys. Rev. B* **38**, 8602 (1988).

⁸See, e.g., A. Abragam and M. Goldman, *Nuclear Magnetism: Order and Disorder* (Clarendon, Oxford, 1982).

⁹Yu. S. Karimov and I. F. Shchegolev, *Zh. Eksp. Teor. Fiz.* **41**,

1082 (1961) [*Sov. Phys. JETP* **14**, 772 (1962)].

¹⁰J. Pointrenaud and J. M. Winter, *J. Phys. Chem. Solids* **25**, 123 (1964).

¹¹D. J. Miller and S. J. Frisken, *J. Appl. Phys.* **64**, 5630 (1988).

¹²B. N. Harmon, X.-W. Wang, and P.-A. Lindgård, *J. Magn. Magn. Mater.* (to be published).

¹³G. J. Ehnholm, J. P. Ekström, M. T. Loonen, and J. K. Soini, *Cryogenics* **19**, 673 (1979).

¹⁴G. J. Ehnholm, J. P. Ekström, J. F. Jacquinot, M. T. Loonen, O. V. Lounasmaa, and J. K. Soini, *J. Low Temp. Phys.* **39**, 417 (1980).

¹⁵P. J. Hakonen and S. Yin, *J. Low Temp. Phys.* **85**, 25 (1991).

¹⁶A. S. Oja, A. J. Annala, and Y. Takano, *J. Low Temp. Phys.* **85**, 1 (1991).

¹⁷P. J. Hakonen, S. Yin, and O. V. Lounasmaa, *Phys. Rev. Lett.* **64**, 2707 (1990).

¹⁸A. Narath, A. T. Fromhold, Jr., and E. D. Jones, *Phys. Rev.* **144**, 428 (1966).